# An Enhanced Chirp Modulated Golay Code for Ultrasound Diverging Wave Compounding

Yanis Mehdi Benane
*Creatis, Univ.Lyon, INSALyon, UCB Lyon 1, UJM-Saint Etienne, CNRS, Inserm,* Lyon, France
yanis.benane@creatis.insa-lyon.fr

Denis Bujoreanu
*Creatis, Univ.Lyon, INSALyon, UCB Lyon 1, UJM-Saint Etienne, CNRS, Inserm,* Lyon, France
denis.bujoreanu@creatis.insa-lyon.fr

Christian Cachard
*Creatis, Univ.Lyon, INSALyon, UCB Lyon 1, UJM-Saint Etienne, CNRS, Inserm,* Lyon, France
christian.cachard@univ-lyon1.fr

Barbara Nicolas
*Creatis, Univ.Lyon, INSALyon, UCB Lyon 1, UJM-Saint Etienne, CNRS, Inserm,* Lyon, France
barbara.nicolas@creatis.insa-lyon.fr

Olivier Basset
*Creatis, Univ.Lyon, INSALyon, UCB Lyon 1, UJM-Saint Etienne, CNRS, Inserm,* Lyon, France
olivier.basset@univ-lyon1.fr

***Abstract*—In ultrasound imaging, a straightforward way of increasing axial resolution is by shortening the transmitted signals. However, short excitation provide low echo signal to noise ratio ($eSNR$), which results in low image quality. An alternate solution would be to increase the excitation signal's duration (by using binary Golay codes or chirps), and rely on off-line match filtering techniques in order to compress the received echoes. Resolution Enhancement Compression (REC) is a coding technique that provides better axial resolution than conventional pulsing technique while increasing the $eSNR$. It consists on designing a pre-enhanced chirp that compensates the most attenuated frequency bands of the ultrasound probe. The objective of this study is to combine orthogonal binary codes with REC pre-enhanced chirps in order to boost further the $eSNR$ provided by REC while keeping its good performance in axial resolution. The method is applied to diverging wave compounding. Pairs of diverging waves are transmitted/received/reconstructed simultaneously thanks to the orthogonality property of the Golay codes. The results show that the proposed method is able to obtain a better image quality than conventional pulse imaging. The axial resolution and the bandwidth was improved by $38\%/15\%$ in simulation/experiment, for an excitation signal designed to provide a $39\%$ boost. The contrast to noise ratio and the $eSNR$ were improved by $3.5dB$ and $18.7dB$ respectively. Acquisition results suggest that the combination between binary codes and modulated enhanced chirps can be implemented in ultrasonic imaging system.**

***Index Terms*—Diverging wave, pulse compression, chirp modulation, resolution enhancement.**

## I. Introduction

Diverging wave ultrasound imaging, as other ultrafast emission schemes that lack beam focusing (plane wave and synthetic aperture imaging), provides a decreased $eSNR$ which limits considerably its penetration depth compared to classical focused ultrasound. This can be a serious drawback in diverging wave applications such as cardiac imaging [1], [2]. Increasing the excitation length could be a solution, however in order to preserve the image resolution one should search for long excitation signals with good pulse compression proprieties. Thus, different types of long excitation signals, with good autocorrelation products (narrow main-lobe, low side-lobes), have already been implemented in ultrasound acquisition schemes. Large number of binary codes [3]–[6] were tested however for now, the signals that yields the best compression (in terms of temporal resolution, signal to noise ratio and side-lobes) are linear frequency modulated signals also called chirps [5]. In [7] and [8], it has been shown that chirps can be further improved in terms of the provided image quality. The main idea is to compensate the effect of the narrow-band ultrasound probe on the chirp during the transmission and echo reception.

Recently, binary Golay codes also gained a vast interest, since these sequences can be compressed without generation of side-lobes [9]. Moreover, groups of mutual orthogonal Golay sequences can be built and emitted simultaneously. In this paper, we propose to combine the advantages of enhanced chirp signals with the orthogonality properties of the Golay sequences. Furthermore, we apply thereby designed signals to a diverging wave compounding imaging technique and evaluate its perfomances by comparing the obtained image quality metrics to the classical way of acquiring diverging waves.

This work was performed within the framework of the ANR-11 TecSan-00801 BBMUT and was supported by LABEX CELYA (ANR-10-LABX-0060) and LABEX PRIMES (ANR-10-LABX-0063), within the program "Investissements d'Avenir" (ANR-11-IDEX-0007) operated by the French National Research Agency (ANR).

## II. Methods

### A. Diverging wave compounding

Let us suppose a linear ultrasound probe placed at $z = 0$ with a total of $N_{el}$ elements (Fig.1). In order to transmit a diverging wave using this probe one should consider a punctual virtual source located at the point $(x_v, z_v)$ with $z_v < 0$. Depending on the region of interest in the medium, which imposes certain angular aperture $\theta$, $n$ elements of the probe are excited with the same excitation $s(t)$ slightly delayed

ISBN 978-90-827970-1-5 © EURASIP 2018

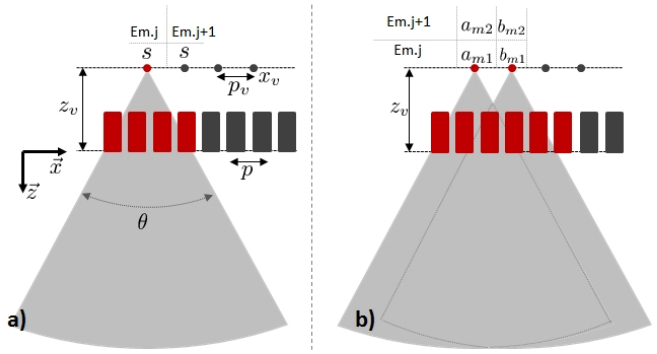


Fig. 1. Transmission schemes used for diverging wave compounding: a) - Classical approach, where $s(t)$ - represents a cycle of a sinusoid, b) - Orthogonal Golay coded approach

depending on the position of each active element. The number of active elements $n$ and the emission delay $t_i$ (for the $i^{th}$ element of the transducer) are determined by [1], [2]:

$$n = \frac{2|z_v|tan(\frac{\theta}{2})}{p} \tag{1}$$

$$t_i = \frac{1}{c}\Big[\sqrt{z_v^2 + (\frac{ip}{2})^2} - z_v\Big] \tag{2}$$

where $i \in \{-n/2, \cdots, n/2-1\}$, $p$ is the pitch of the ultrasound probe and $c$ is the propagation speed of sound in soft tissues.

After one diverging wave transmission, the received echoes are recorded and beamformed in either time or frequency domain [2]. Envelope extraction and log-compression is performed on the resulting radio frequency image.

In order to increase the signal to noise ratio and to further widen the region of interest, it was proposed in [1] to do diverging wave compounding. The main idea is to consider that $N_{dw}$ virtual sources are located behind the real ultrasound probe. Each virtual source $j$ has a position defined by $(x_{jv}, z_v)$ where $x_{jv} = jp_v$, $p_v$ being the pitch of the virtual transducer. The reconstruction pipeline for the final compounded image can be divided in the following steps:

(a) activate virtual source $j$
(b) compute, using (1), the corresponding $n$ elements of the ultrasound probe to be activated
(c) compute the transmission delays for each $i^{th}$ active element of the probe by adapting (2) to:

$$t_i^j = \frac{1}{c}\Big[\sqrt{z_v^2 + \big(x_{jv} + \frac{ip}{2}\big)^2} - z_v\Big] \tag{3}$$

with $i \in \{-n/2, \cdots, n/2-1\}$
(d) transmit the diverging wave (Em.$j$ on Fig.1a)
(e) receive the backscattered echoes and do the beamforming to obtain a low resolution image
(f) repeat steps $a$ to $e$ for $j \in \{1, \cdots, N_{dw}\}$
(g) add all the low resolution images to obtain the final image.

### *B. Orthogonal Golay Coded Diverging Wave Compounding*

Complementary Golay coded transmission signals are already used in a large number of imaging techniques [10], [12] however their orthogonality properties seem to be explored only in a few [9], [13]. In this section, we present the first implementation of the mutually orthogonal Golay sets to diverging wave compounding.

Let us suppose a set of two Golay complementary sequences of length $n = 8$, $(a_1, a_2)$, with $a_i(k) \in \{-1, +1\}$. The complementarity property of $a_1$ and $a_2$ implies that:

$$R_{a_1a_1}(k) + R_{a_2a_2}(k) = 2n\delta(k) \tag{4}$$

where $\delta(k)$ is the Kronecker delta function and $R_{a_1a_1}(k)$ ($R_{a_2a_2}(k)$) represents the autocorrelation products of the sequence $a_1$ ($a_2$) respectively. As it was shown in [14], it is possible to build from $(a_1, a_2)$ a mate set $(b_1, b_2)$ that has the following 3 properties: i) $b_1$ and $b_2$ are of the same length ($n$) as $a_1$ and $a_2$ respectively; ii) the set $(b_1, b_2)$ is complementary, thus follows (4); iii) the sets $(a_1, a_2)$ and $(b_1, b_2)$ are mutual orthogonal meaning that :

$$\sum_{j=1}^{2} R_{a_jb_j}(k) = 0, \forall k \tag{5}$$

where $R_{a_jb_j}(k)$ represents the intercorrelation product between the sequences $a_j$ and $b_j$.

Now, in order to transmit a diverging wave that carry a binary sequence $a_j$ (or $b_j$), one should modulate them with a signal $r(t)$ whose frequency content falls inside the bandwidth of the ultrasound probe. Different carriers $r(t)$ were proposed [5], [10] such as half or full period of a sinusoid, square wave or chirps. The choice of the carrier is very complex since there is an inherent trade-off between the echo signal to noise ratio and the resolution of the reconstructed image [10]. The resulting modulated signals $a_{mj}(t)$, $b_{mj}(t)$ can be written as:

$$\begin{aligned} a_{mj}(t) &= \sum_{k=0}^{n-1} a_j(k)\delta\Big(t - kT\Big) * r(t) \\ b_{mj}(t) &= \sum_{k=0}^{n-1} b_j(k)\delta\Big(t - kT\Big) * r(t) \end{aligned} \tag{6}$$

where $\delta(t)$ is the Dirac delta function and $T$ is the time duration of the carrier $r(t)$. Assuming that the backscattered echoes are exact copies of $a_{mj}(t)$ and respectively $b_{mj}(t)$ (with less amplitude due to the geometrical spreading of the wave), from (4) and (6) is obtained the expression of the pulse compressed waveforms:

$$\begin{aligned} R_{a_{m1}a_{m1}}(t) + R_{a_{m2}a_{m2}}(t) &= 2n\big[r(t) * r(-t)\big] \\ R_{b_{m1}b_{m1}}(t) + R_{b_{m2}b_{m2}}(t) &= 2n\big[r(t) * r(-t)\big] \end{aligned} \tag{7}$$

In (7), it can be seen that the quality of the compressed waveforms depends on the autocorrelation product of the carrier signal $r(t)$. Furthermore, using (5) and (6) it can be also deduced that:

$$\sum_{j=1}^{2} R_{a_{mj}b_{mj}}(t) = 0, \forall t \tag{8}$$

which in other words means that the modulated sets $(a_{m1}, a_{m2})$ and $(b_{m1}, b_{m2})$ are also mutually orthogonal.

In order to use the above described properties of $(a_{m1}, a_{m2})$ and $(b_{m1}, b_{m2})$ in diverging wave compounding, we propose the following pipeline:

ISBN 978-90-827970-1-5 

(a) consider virtual source $j$ and $j+1$
(b) compute, using (1), the corresponding $n$ elements of the ultrasound probe to be activated for $j$ and $j+1$
(c) compute, using (3), the emission delays for the $i^{th}$ active element of the probe for $j$ and $j+1$
(d) transmit simultaneously with the source $j$: $a_{m1}(t)$ and with the source $j+1$: $b_{m1}(t)$ (Em.$j$ in Fig.1b)
(e) receive the backscattered echoes at each $i$ element of the probe: $y_{1i}(t)$
(f) transmit simultaneously with the source $j$: $a_{m2}(t)$ and with the source $j+1$: $b_{m2}(t)$ (Em.$j+1$ in Fig.1b)
(g) receive the backscattered echoes at each $i$ element of the probe: $y_{2i}(t)$
(h) compress the the received echoes at the steps $e$ and $g$ as in (7) by applying the corresponding matched filters:

$$\begin{aligned}\hat{g}_j(t) &= y_{1i}(t) * a_{m1}(-t) + y_{2i}(t) * a_{m2}(-t)\\ \hat{g}_{j+1}(t) &= y_{1i}(t) * b_{m1}(-t) + y_{2i}(t) * b_{m2}(-t)\end{aligned} \tag{9}$$

(i) beamform the compressed signals $\hat{g}_j(t)$ and $\hat{g}_{j+1}(t)$ in order to obtain simultaneously the low resolution images (corresponding to a successive emission with the virtual source $j$ and $j+1$)
(j) repeat steps $a$ to $i$ $N_{dw}/2$ times, increasing $j$ with a step of 2
(k) add all the low resolution images to get the final image.

### C. Chirp modulated orthogonal coded diverging wave

As mentioned in section II.B, depending on the modulation signal $r(t)$ in (6), for the same lengh $n$ of the Golay sequences, the resulting compressed echoes have either a good temporal resolution ($T$ decreases) or a good echo signal to noise ratio ($T$ increases). Nevertheless, recent work [5] has shown that it is possible to combine complementary Golay sequences with chirp signals (Fig.2b) in order to increase the echo signal to noise ratio for a small loss of temporal resolution (Fig.2). However, as it was shown in [7], a narrow band ultrasound probe can downgrade the quality of the autocorrelation of a chirp signal by increasing the compression side-lobes and decreasing the temporal resolution.

In this work, we propose to improve the above described chirp modulation technique, by compensating the effects of the narrow band ultrasound probe using a technique called Resolution Enhancement Compression (REC) [7], [8]. REC can improve the temporal resolution even with a narrow band probe. One of the central aspects of REC is the generation of an excitation signal referred to as pre-enhanced chirp. This chirp can artificially enlarge the bandwidth of the transducer, thereby providing higher axial resolution. The core principle on which REC relies in the following convolution equivalence:

$$v_{rec}(t) * h_1(t) = v_{lin}(t) * h_2(t) \tag{10}$$

where, as shown in Fig.2, $h_1(t)$ is the pulse-echo impulse response of a probe element at its focal length, $h_2(t)$ describes the designed pulse-echo impulse response with such desired properties as larger spectral support and $v_{lin}(t)$ is a chirp that covers the bandwidth of $h_2(t)$.

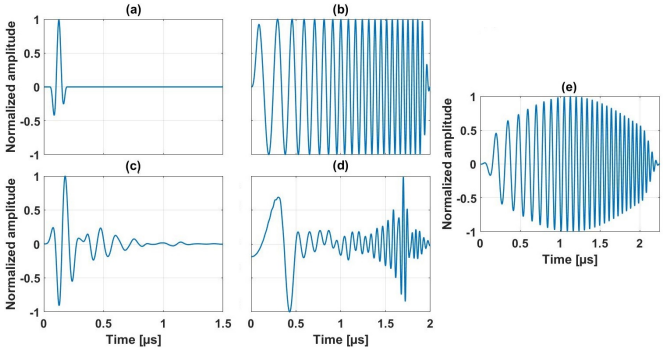


Fig. 2. a) - Desired pulse-echo impulse response $h_2(t)$, b) - $v_{lin}(t)$, chirp used for modulation of the Golay codes in [5], c) - Pulse-echo impulse response of the probe $h_1(t)$, d) - $v_{rec}(t)$, chirp used for modulation of the Golay codes in our approach, e) - Result of the convolution expression (10).

The probe elements are excited with a frequency and amplitude modulated waveform $v_{rec}(t)$ called pre-enhanced chirp. Equation (10) suggests that by exciting the probe that has a narrow bandwidth with the pre-enhanced chirp, this transducer can yield the same axial resolution as a probe with a larger bandwidth when it is excited by a simple linear chirp, thereby resulting into a higher axial resolution. By solving (10) in the frequency domain, the pre-enhanced chirp is obtained:

$$V_{REC}(f) = V_{LIN}(f) \times \frac{H_2(f)}{H_1(f)} \tag{11}$$

where the capital letters represent the Fourier transforms of the corresponding temporal signals. In order to obtain a good approximation of $v_{rec}(t)$, Oelze [7] proposed to replace $H_2(f)/H_1(f)$ by a Wiener filter. $V_{REC}(f)$ becomes:

$$V_{REC}(f) = V_{LIN}(f) \times \frac{H_1^*(f)H_2(f)}{|H_1(f)|^2 + |H_1(f)|^{-2}} \tag{12}$$

where $()^*$ denotes complex conjugation. $v_{rec}(t)$ was multiplied with a Tukey-cosine window with a 20% taper in order to reduce side-lobe levels. The full generation process of the signal $v_{rec}(t)$ is presented in the Fig.2.

Where in the classical chirp modulation of the Golay codes [5], the signal illustrated in Fig.2b is used, we propose to use for modulation $v_{rec}(t)$ (Fig.2d). This modulation can be achieved by replacing, in (6), $r(t)$ with $v_{rec}(t)$. In Fig.3 is

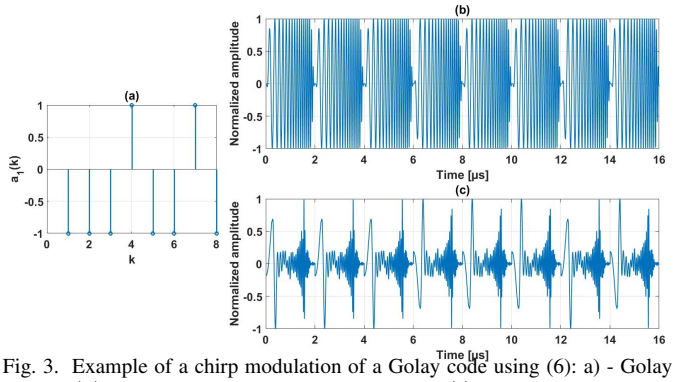


Fig. 3. Example of a chirp modulation of a Golay code using (6): a) - Golay code $a_1(k)$, b) - Modulated Golay code using $v_{lin}(t)$, c) - Modulated Golay code using $v_{rec}(t)$

ISBN 978-90-827970-1-5 

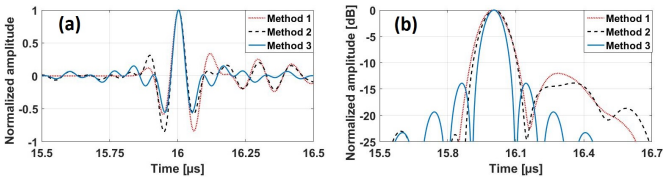


Fig. 4. a) - Signal obtained after echo compression using (9), b) - Envelope of the beamformed radiofrequency data

presented the process of modulating the Golay code ($n = 8$) $a_1(t) = \{-1, -1, -1, 1, -1, -1, 1, -1\}$.

An illustration of the compressed waveforms of the chirp modulated signals (Fig.3b and c) is displayed in Fig.4a. Fig.4b shows that the designed chirp $v_{rec}(t)$, used for Golay code modulation yields $37\%$ better temporal resolution than $v_{lin}(t)$. Moreover, Fig.4b shows that the proposed method increases also the temporal resolution (after compression) even compared to classical approach, where the probe excitation signal $s(t)$ is a cycle of a sinusoid at the center frequency of the probe bandwidth: $39\%$ boost is achieved.

## III. Simulation results

A linear probe with 192 elements and a pitch of $0.245mm$ was used for simulations. The center frequency and sampling frequency were $8.5MHz$ and $61.6MHz$, respectively. To assess the perfomance of the studied methods (in terms of axial resolution, bandwidth and echo signal to noise ratio ($eSNR$)) a resolution phantom from the Plane-wave Imaging Challenge in Medical UltraSound (PICMUS) dataset [15] was simulated using Field II [11]. The contrast to noise ratio (CNR) and the speckle size were measured on B-mode images obtained from simulations on a cyst phantom from the Field II database. A white Gaussian noise ($SNR = 20dB$) was added into the channel data before pulse compression and beamforming were performed. Three acquisition methods using diverging wave compounding ($N_{dw} = 40$, $z_v = -1cm$, $x_v \in [-2 \cdots 2]cm$) were compared. Method I: Conventional approach, where the excitation signal is a period of a sinusoid. Method II: Orthogonal Golay coded, where the codes are modulated with $v_{lin}(t)$. Method III (proposed approach): Orthogonal Golay coded, where the codes are modulated with $v_{pre}(t)$.

### A. Resolution phantom results

The obtained B-mode images for the different techniques are shown in Fig.5. It can be visually observed that Method III shows a better axial resolution and lower background noise. As shown in Fig.6a, the improvement concerning the axial resolution is quantified through the envelope of the beamformed radiofrequency signals (at $-6dB$). The measured values are $133.1\mu m$, $130.9\mu m$ and $96\mu m$ for Method I, Method II and Method III respectively.

The power spectra of the reflection from the wire at $4cm$ depth is shown in Fig.6b. In accordance with the improvement in axial resolution, the $-6dB$ bandwidths were $5.14MHz$, $5.22MHz$ and $7.16MHz$ for Method I, Method II and Method III respectively. Concerning the $eSNR$ calculated on the pre-beamformed data, a higher value is obtained in

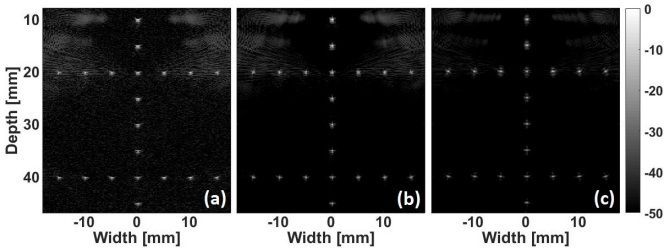


Fig. 5. Obtained B-mode images: a) Method I, b) Method II, c) Method III

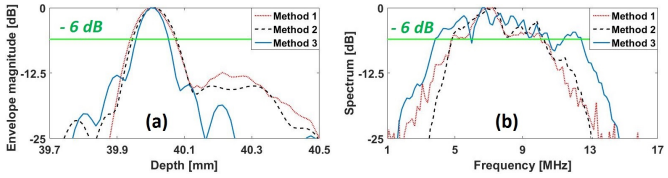


Fig. 6. a) - Envelope of the beamformed radiofrequency data, b) - Normalized spectrum from the beamformed radiofrequency data

Method II ($48.7dB$) than Method III ($40.1dB$), Method I providing the lowest value ($21.4dB$). The obtained values are consistent with the expected ones, the difference of $8.6dB$ between Method II and III being explained by the modulated shape of the excitation in Method III (Fig.2d), that carries approximatively $2.8$ times less energy than the chirp used for Method II emission (Fig.2b).

### B. Cyst phantom results

The obtained B-mode images are shown in Fig.7. These results show an improvement in terms of image quality between Method III (Fig.7c) compared to Method I and Method II (Fig.7a and b). The CNR, defined as $|\mu_{ROI} - \mu_{back}|/\sqrt{\sigma^2_{ROI} + \sigma^2_{back}}$, where $ROI$ stands for the region of interest (cyst) and $back$ stands for the background around the cyst. The obtained values for the hypo-echoic (hyper-echoic) were $-4.11dB$, $-2.48dB$, $1.51dB$ ($-8.21dB$, $-8.23dB$, $9.46dB$) for Method I, Method II and Method III respectively.

The speckle axial size was also evaluated through autocorrelation length (ACL) which consists in calculating the autocorrelation product of a vertical beamformed radio-frequency line. The ACL results in Fig.8 (Method I $474.4\mu m$, Method II $505.9\mu m$, Method III $364.6\mu m$) show an improvement of $30\%$ between Method III/Method I and $39\%$ between Method III/Method II. The improved speckle size, provided by Method

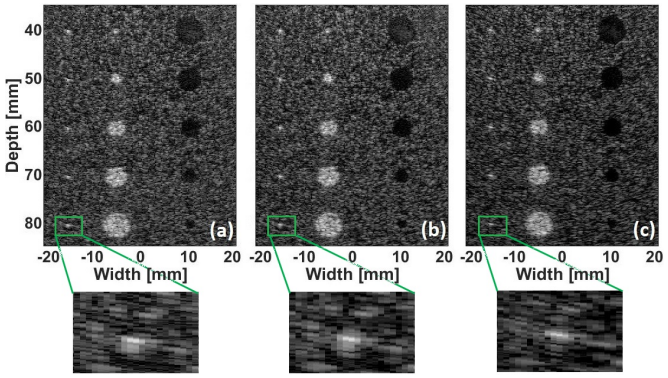


Fig. 7. Obtained B-mode images: a) Method I, b) Method II, c) Method III

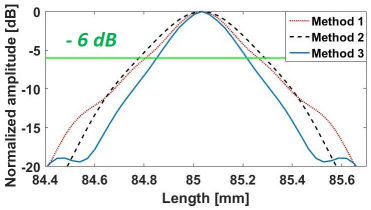


Fig. 8. Autocorrelation length in the axial direction performed on the vertical line at $3mm$ in the cyst B-mode image

III, is in accordance with the boost of axial resolution observed on the scatterer placed at $(x, z) = (-15, 80)mm$ (see zoomed zone in Fig.7). We measure a boost of $29.2\%$ and $37.5\%$ for Method III/Method I and Method III/Method II respectively.

## IV. Experimental results

For the data acquisition, the open ultrasound platform UlaOp 256 (Microelectronics System Design Lab, Florence, Italy) [16] equipped with a LA523E-array probe (Esaote, Genova, Italy) was used. The UlaOp 256 is able to transmit arbitrary waveforms and defined specific transmission/reception strategies. The probe has 192 elements ($pitch = 245\mu m$) and is centered at $8.5MHz$. The phantom studied (model 410SCG HE 0.5 Gammex Sun nuclear, Neu-Isenburg, Germany) has an attenuation coefficient slope of $0.5dB/MHz/cm$. The obtained log compressed B-mode images for the three studied methods are displayed in Fig.9.

The results clearly show an improvement in term of CNR between Method III (Fig.9c) and Method I (Fig.9a). Indeed the obtained values are $7.4dB$ and $3.9dB$ respectively. The difference of CNR between Method III and Method II (Fig.9b) is only of $0.2dB$. The discrepancy, in comparison to the simulation results in CNR, is due to the effect of attenuation that alters the received echoes more for Method III than Method II since the Method III excitation signals content more high frequency (due to enhancement of the bandwidth).

As it can be seen in Fig.10a, a better axial resolution is obtained using Method III than Method I and II. $14\%$ and $29.4\%$ of enhancement is achieved between Method III/Method I ($228.2\mu m$/$260.1\mu m$) and Method III/Method II ($228.2\mu m$/$295.2\mu m$) respectively. The axial autocorrelation length measurement (Fig.10b) is consistent with the obtained axial resolution values and show a $15\%$ and $34.4\%$ boost for Method III/Method I and Method III/Method II respectively.

## V. Conclusion

In this study, the first experimental implementation of enhanced chirp modulation of orthogonal Golay codes (Method III) is presented. In comparison with conventional imaging technique (Method I) and classical chirp modulation of orthogonal Golay codes (Method II), the results show improvements in terms of image quality as quantified by the CNR, axial resolution, bandwidth and speckle size. The experimental results suggest that the combination between binary Golay codes and per-enhanced modulated chirps is feasible and provide advantages for imaging when implemented on narrow-band ultrasound probes.

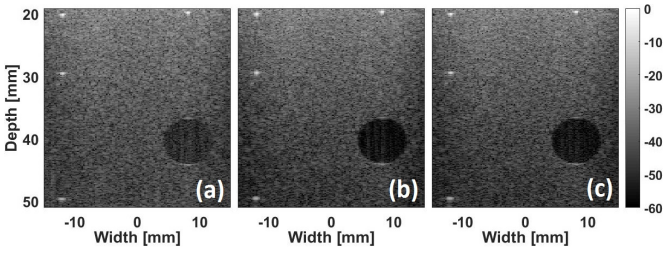


Fig. 9. Obtained B-mode images: a) Method I, b) Method II, c) Method III

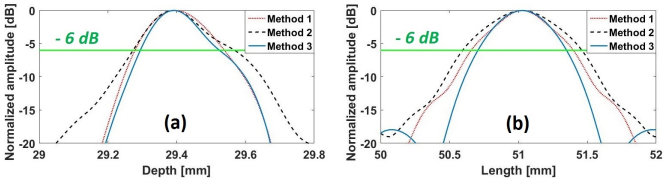


Fig. 10. a) - Envelope of the beamformed radiofrequency data, b) - Autocorrelation length in the axial direction performed on the vertical line at $3mm$ in the cyst B-mode image

## References

[1] C. Papadacci, M. Pernot, M. Couade, M. Fink, and M. Tanter, "High contrast ultrafast imaging of the heart," IEEE TUFFC, vol. 61, no. 2, pp. 288-301, 2014.

[2] M. Zhang, F. Varray, A. Besson, R. E. Carrillo, M. Viallon, D. Garcia, O. Bernard, "Extension of Fourier-based techniques for ultrafast imaging in ultrasound with diverging waves," IEEE TUFFC, vol. 63, no. 12, pp. 2125-2137, 2016.

[3] F. Gran, J. A. Jensen, "Spatial encoding using a code division technique for fast ultrasound imaging," IEEE TUFFC, vol. 55, no. 1, 2008.

[4] D. Bujoreanu, H. Liebgott, and B. Nicolas,"Simultaneous coded plane wave imaging in ultrasound: Problem formulation and constraints," IEEE ICASSP, 2017.

[5] B. Lashkari, K. Zhang, A. Mandelis, "High-frame-rate synthetic aperture ultrasound imaging using mismatched coded excitation waveform engineering: A feasibility study," IEEE TUFFC, vol. 63 no.6, pp. 828-841, 2016.

[6] E. Tiran, T. Deffieux, M. Correia, D. Maresca, B.F. Osmanski, L.A. Sieu, M. Tanter, "Multiplane wave imaging increases signal-to-noise ratio in ultrafast ultrasound imaging" IOP PMB, vol. 60, no. 21, pp. 8549, 2015.

[7] M. L. Oelze, "Bandwidth and resolution enhancement through pulse compression," IEEE TUFFC, vol. 54, no. 4. pp. 768-781, 2017.

[8] Y. M. Benane, R. Lavarello, D. Bujoreanu, C. Cachard, F. Varray, A. S. Savoia, O. Basset, "Ultrasound bandwidth enhancement through pulse compression using a CMUT probe," IEEE IUS, pp. 1-4, 2017.

[9] I. Trots, "Mutually Orthogonal Golay Complementary Sequences in Synthetic Aperture Imaging Systems," Archives of Acoustics, vol. 40, no. 2, pp. 283-289, 2015.

[10] A. Nowicki, I. Trots, P. A. Lewin, W. Secomski, and R. Tymkiewicz, "Influence of the ultrasound transducer bandwidth on selection of the complementary Golay bit code length," Ultrasonics, vol. 47, no. 14, pp. 64-73, 2007.

[11] J. A. Jensen, "Field: A program for simulating ultrasound systems," in 10th Nordicbaltic Conference on Biomedical Imaging, supplement 1, part 1, vol. 4, pp. 351-353, 1996.

[12] J. Liu, M. F. Insana, "Coded pulse excitation for ultrasonic strain imaging," IEEE TUFFC, vol. 52, no. 2, pp. 231-240, 2005.

[13] B. H. Kim, T. K. Song, "Multibeam Simultaneous Transmit Multizone (MB-STMZ) focusing method using modulated orthogonal codes for ultrasound imaging," Med. Imag. UIASP, vol. 5373, pp. 315-324, 2004.

[14] C.C. Tseng, C. Liu, "Complementary sets of sequences," IEEE Transactions on Information theory, vol. 18, no. 5, pp. 644-652, 1972.

[15] H. Liebgott, A. R-Molares, J. A. Jensen, O. Bernard, "Plane-Wave Imaging Challenge in Medical Ultrasound", IEEE IUS, pp. 1-4, 2016.

[16] E. Boni, L. Bassi, A. Dallai, F. Guidi, V. Meacci, A. Ramalli, P. Tortoli, "ULA-OP 256: A 256-channel open scanner for development and real-time implementation of new ultrasound methods," IEEE TUFFC, vol. 63, no. 10, pp. 1488-1495, 2016.

ISBN 978-90-827970-1-5 © EURASIP 2018